Panovska, S., Constable, C. (2017): An activity index for geomagnetic paleosecular variation, excursions, and reversals. - *Geochemistry Geophysics Geosystems (G3)*, *18*, 4, pp. 1366—1375.

DOI: http://doi.org/10.1002/2016GC006668

AGU PUBLICATIONS

Geochemistry, Geophysics, Geosystems

RESEARCH ARTICLE
10.1002/2016GC006668

An activity index for geomagnetic paleosecular variation, excursions, and reversals

S. Panovska[1,2] and C. G. Constable[1]

[1]Institute of Geophysics and Planetary Physics, Scripps Institution of Oceanography, University of California, San Diego, California, USA, [2]Now at Helmholtz-Zentrum Potsdam, Deutsches GeoForschungsZentrum, Telegrafenberg, Potsdam, Germany

Key Points:
- New PSV index for characterization of modern and paleomagnetic secular variation, geomagnetic excursions, and reversals is introduced
- Transitional events—geomagnetic excursions and polarity reversals—are characterized by PSV index larger than 0.5
- The PSV activity index, defined as the temporal standard deviation of the PSV index, provides a measure of geomagnetic field stability

Supporting Information:
- Supporting Information S1
- Data Sets S1–S8

Correspondence to:
S. Panovska,
sanja.panovska@gfz-potsdam.de

Citation:
Panovska, S. and C. G. Constable (2017), An activity index for geomagnetic paleosecular variation, excursions, and reversals, *Geochem. Geophys. Geosyst.*, *18*, 1366–1375, doi:10.1002/2016GC006668.

Received 6 OCT 2016
Accepted 23 FEB 2017
Accepted article online 28 FEB 2017
Published online 3 APR 2017

Abstract Magnetic indices provide quantitative measures of space weather phenomena that are widely used by researchers in geomagnetism. We introduce an index focused on the internally generated field that can be used to evaluate long term variations or climatology of modern and paleomagnetic secular variation, including geomagnetic excursions, polarity reversals, and changes in reversal rate. The paleosecular variation index, P_i, represents instantaneous or average deviation from a geocentric axial dipole field using normalized ratios of virtual geomagnetic pole colatitude and virtual dipole moment. The activity level of the index, σ_{P_i}, provides a measure of field stability through the temporal standard deviation of P_i. P_i can be calculated on a global grid from geomagnetic field models to reveal large scale geographic variations in field structure. It can be determined for individual time series, or averaged at local, regional, and global scales to detect long term changes in geomagnetic activity, identify excursions, and transitional field behavior. For recent field models, P_i ranges from less than 0.05 to 0.30. Conventional definitions for geomagnetic excursions are characterized by P_i exceeding 0.5. Strong field intensities are associated with low P_i unless they are accompanied by large deviations from axial dipole field directions. σ_{P_i} provides a measure of geomagnetic stability that is modulated by the level of PSV or frequency of excursional activity and reversal rate. We demonstrate uses of P_i for paleomagnetic observations and field models and show how it could be used to assess whether numerical simulations of the geodynamo exhibit Earth-like properties.

1. Introduction

Earth's magnetic field is derived from a broad array of physical processes with multiple characteristic time scales, ranging from the geodynamo in Earth's core, through the atmosphere, ionosphere, and magnetospheric interactions with the solar wind. Our knowledge of these processes is necessarily incomplete, and for the external parts of the geomagnetic field led to the introduction of several geomagnetic indices to serve as a reference for geophysical processes and to describe the properties of short term geomagnetic variations [e.g., *Mayaud*, 1980]. Geomagnetic indices, such as Dst, K, Kp and AE, have been used since the early twentieth century to characterize activity in the external part of the modern geomagnetic field, which is important in many subdisciplines of geomagnetism, allowing, for example, explicit rules for exclusion of disturbed data in internal field modeling [e.g., *Olsen et al.*, 2006], in addition to being a diagnostic for space weather [*Love and Remick*, 2007]. For instance, the hourly storm-time disturbance index Dst [*Sugiura*, 1964] is calculated from the horizontal intensity data recorded at near-equatorial geomagnetic observatories and measures the intensity of the magnetospheric ring current system. The K index measures the storm magnetic activity for separate geomagnetic observatories, while the planetary Kp averages the K indices at 13 subauroral observatories [*Menvielle and Berthelier*, 1991]. The auroral electrojet index AE, a measure of the auroral zone magnetic activity, is calculated from the intensities of the eastward and westward auroral electrojets [*Davis and Sugiura*, 1966]. Hence, these indices reflect regional and global manifestations of external activity and serve as proxies for describing the associated physical processes. However, no adequate simple diagnostics exist yet for the internal geomagnetic field that originates in Earth's liquid outer core. Recent efforts in both paleomagnetic data gathering and modeling activity suggest that a basic means of characterizing the internal geomagnetic weather/climate and its longer term variability would also be useful, and that is the goal of this paper.

Specifically, we propose a paleosecular variation (PSV) index, useful as both a local and global measure of field state whose temporal variability can be used to measure secular variation activity during stable polarity

times when the field is dominated by an axial dipole; it also serves as a means of identifying more extreme behavior associated with geomagnetic excursions and reversals, and as a proxy for long term nonstationary field behavior, like changes in reversal rate. The rather frequent occurrence of transitional directions and low field strength associated with reversals and excursions during the Quaternary has stimulated the development of a chronological tool known as the geomagnetic instability time scale [*Singer*, 2014]. However, it remains unclear how such instabilities emerge from more typical paleosecular variation, in part because of a lack of adequate diagnostics. In geodynamo simulations, the transition region between the stable dipolar regime and multipolar regime has been characterized by a parameter called local Rossby number—the ratio of inertial to Coriolis effects in the outer core fluid motions. This transition is found to occur when the local Rossby number is around 0.12 [*Olson and Christensen*, 2006; *Wicht et al*., 2009]. A general PSV index and improved understanding of characteristic activity levels will also provide a new tool for linking empirical paleomagnetic observations to physical processes and their proxy characterizations in Earth-like geodynamo simulations.

In paleomagnetism, the colatitude of the virtual geomagnetic pole (VGP) has long been used as a measure of deviation from a geocentric axial dipole configuration for the field. VGP dispersion about the geographic axis in paleomagnetic records from lava flows, and more specifically its variation with latitude, provides an estimate of root mean square (rms) directional field variability due to PSV [e.g., *Merrill et al*., 1996]. Proxy values are often considered to provide a useful means of determining whether secular variation has been averaged out before producing paleomagnetic poles for plate reconstruction [e.g., *Butler*, 1992]. But *McFadden et al*. [1988] also noted that the increase in average VGP dispersion with latitude could be a product of equatorially antisymmetric field contributions to the PSV, while equatorially symmetric contributions set the base level of VGP dispersion at the equator. *McFadden et al*. [1991] found a relationship between the reversal frequency and the absolute latitudinal dependence of VGP dispersion in paleomagnetic data from lava flows, and inferred that a relative increase in symmetric contributions led to destabilizing the field. However, no link to overall field intensity was available. Based on geodynamo simulations, *Coe and Glatzmaier* [2006] suggested an inverse correlation between the geomagnetic field stability and equatorial symmetry of the field that is consistent with paleomagnetic observations. Equatorially antisymmetric contributions are associated with terms in a spherical harmonic representation for which the sum of degree (l) and order (m) is odd, while symmetric terms have $l + m$ even. They introduced an empirical measure of the relative contribution of odd to even harmonics, calculated as a ratio of their spatial energy density contributions. The more antisymmetric the field is, the more stable it is, with low reversal frequency. The advantage of this prescription is that it brought field strength into the characterization, but because the method relies on the field being given in a spherical harmonic representation it is difficult to apply to empirical paleomagnetic observations on a local or regional scale.

A particular question that can be addressed by geographic variations in an index that characterizes the internal geomagnetic field is hemispheric asymmetry in the field structure, whether North/South or Atlantic/Pacific on different time scales and time averages. For example, *Jackson et al*. [2000] observed a higher level of secular variation in the Atlantic with respect to the Pacific in historical geomagnetic field. Results on longer time scales (10^6 years and greater) are not yet definitive [*Cromwell et al*., 2015] but suggest the possibility of north-south asymmetries [*Cromwell et al*., 2012, 2013]. Recently, *Ziegler and Constable* [2015] observed visible regional differences in paleointensity reconstructions over the past 300 kyr. Global variations in both average virtual axial dipole moment (VADM) and its standard deviation about the mean for recent time-averaged 0–10 kyr field models CALS10k.2 and HFM.OL1.A1 [*Constable et al*., 2016] also show significant spatial differences.

Geomagnetic excursions have usually been identified by VGPs deviating more than some conventional limit from the geographic pole (often 45 degrees), and/or by periods of significant intensity drops below some critical value, for example, 50% of the present-day field. The link between low intensity and VGP colatitude has been examined, for example, by *Lu Lin et al*. [1994] who found a correlation between the logarithm of the virtual dipole moment and the VGP colatitude during geomagnetic excursions and reversals.

We seek a quantitative definition of excursional behavior in paleomagnetic records by searching for emerging synchronous directional deviations and lows in paleointensity. Geographic and temporal variations in each of these properties carry information about equatorial and other symmetry properties. In section 2, we combine paleointensity signals in the form of virtual dipole moment (VDM) with virtual geomagnetic pole

positions in a single parameter, which we call the PSV index, P_i. This diagnostic can be evaluated for any geomagnetic time series (individual data records, model predictions, spherical harmonic coefficients, etc.) to characterize the level of paleosecular variation activity, find excursions, or even study incipient reversals.

A baseline for the new index is established using modern and historic geomagnetic field models to analyze stable field configurations: Swarm Initial Field Model (SIFM) for 2014 [*Olsen et al*., 2015], International Geomagnetic Reference Field (IGRF-12) [*Thébault et al*., 2015], and *gufm1* which spans 1590–1990 AD [*Jackson et al*., 2000] are used. The most striking feature of the present geomagnetic field, the South Atlantic Anomaly (SAA), is of great interest to the scientific community because of continuing speculation that Earth could be heading toward a field reversal [*Hulot et al*., 2002; *Olson et al*., 2009; *De Santis and Qamili*, 2015]. This feature is an area of low magnetic field strength spanning the South Atlantic, produced by a patch of reverse magnetic flux in the outer core identified in analyses of modern field data. We compare the PSV indices of the SAA with values for transitional events, excursions, and reversals derived from both sedimentary paleomagnetic records, and from numerical simulations covering long time scales.

2. Methodology

A basic transformation widely used in paleomagnetism is the unique mapping of a local vector magnetic field measurement, **B**, at a site location with latitude and longitude, (λ_s, ϕ_s), into an equivalent geocentric dipole vector, **M**. **M** has magnitude, *M* (the VDM), and the location, (λ_p, ϕ_p), where its axis pierces Earth's surface is the VGP. Although VGP and VDM are often thought to be based on the assumption that **B** has been produced by a dipolar geomagnetic field, all the nondipole contributions in the magnetic field components are carried through the site dependent transformation [e.g., *Constable*, 2003]. Therefore, *M*, λ_p, and ϕ_p can be employed to describe the geomagnetic field at site location λ_s, ϕ_s during both stable and transitional periods.

In paleomagnetic studies, it is often the case that full vector information is not available, either only directional (inclination *I*, declination *D*) or only intensity data, *F*, and correspondingly, one of the two basic nonlinear transformations of local paleomagnetic directions or intensity data are used to produce VGPs and VDMs. These form the basis for evaluating P_i, as described below. Magnetic poles have broad uses in the paleomagnetic community, for example, in comparisons between various observation sites, analyses of geomagnetic excursions or reversals, and in plate reconstructions, while dipole moments provide a basic measure of field strength.

A virtual geomagnetic pole position (λ_p, ϕ_p) is calculated from geomagnetic directions measured at a particular site with geographic coordinates (λ_s, ϕ_s), as follows. The magnetic colatitude *p* can be calculated from the dipole formula [*Butler*, 1992]:

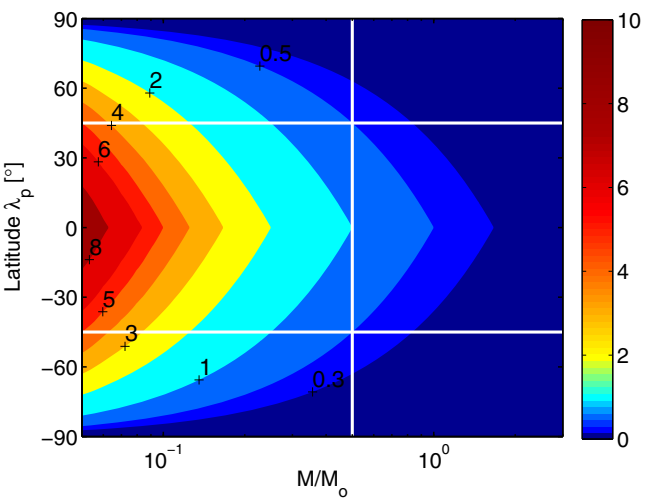

Figure 1. Values of PSV index across the plausible range of VDM and VGP latitudes. Intersections of the white lines represent the conventional limit used to characterize geomagnetic excursions, a PSV index value of 0.5.

$$p = \tan^{-1}\left(\frac{2}{\tan I}\right) \quad (1)$$

Using spherical trigonometry, the pole latitude is given by

$$\lambda_p = \sin^{-1}(\sin\lambda_s \cos p + \cos\lambda_s \sin p \cos D) \quad (2)$$

The strength associated with the VGP is given by the VDM, *M*, which is determined from the measured or predicted intensity, *F*, by the equation [e.g., *Constable*, 2007]:

$$M = \frac{4\pi a^3}{\mu_0}\frac{F}{\sqrt{1+3\cos^2 p}} \quad (3)$$

where *a* is the average radius of the Earth, μ_0 is the permeability of free space, and *p* is magnetic colatitude

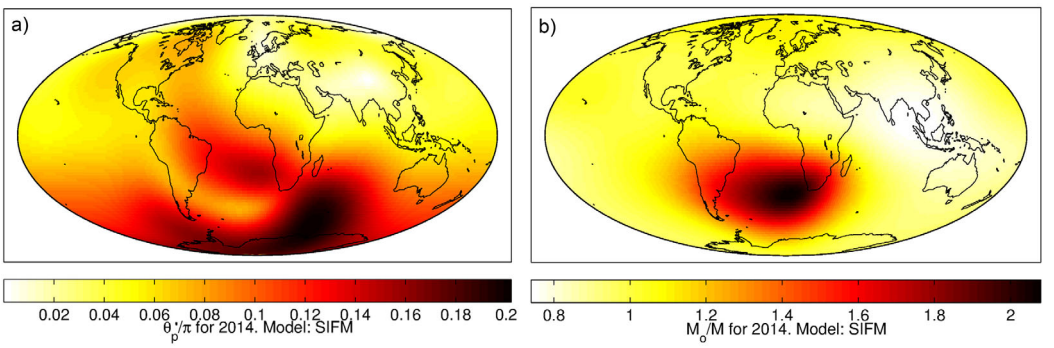

Figure 2. PSV index analysis of SIFM for 2014: Maps of the (a) directional component $(\pi/2-|\lambda_p|)/\pi$ and (b) dipole moment component M_0/M. Pointwise multiplication of values on these two maps produces the index presented in Figure 3a.

(equation (1)). Using the VDM (as opposed to the VADM) ensures that no scatter is introduced by the virtual dipole wobble already represented by the VGP, because the magnetic colatitude is independent of the orientation of the dipole relative to the Earth's axis of rotation [*Merrill et al.*, 1996]. And as we saw above in the case of full vector records the VDM, M, is the magnitude of the unique dipole vector directly associated with calculation of VGP from directional and intensity data.

The PSV index is defined as follows:

$$P_i(\lambda,\phi,t)=\frac{(\pi/2-|\lambda_p(\lambda,\phi,t)|)/\pi}{M(\lambda,\phi,t)/M_0}=\frac{(\pi/2-|\lambda_p(\lambda,\phi,t)|)\,M_0}{\pi\,M(\lambda,\phi,t)} \tag{4}$$

where λ_p is the local VGP latitude at latitude λ, longitude ϕ, and time t, and M is the corresponding virtual dipole moment. The absolute deviation of λ_p from the geographic pole and the virtual dipole moment are scaled by π and the approximate present day dipole moment $M_0=80\,\mathrm{ZAm}^2$ to provide a nondimensional index. Alternatively, the PSV index can be expressed as:

$$P_i(\lambda,\phi,t)=\frac{\theta'_p(\lambda,\phi,t)/\pi}{M(\lambda,\phi,t)/M_0}=\frac{\theta'_p(\lambda,\phi,t)\,M_0}{\pi\,M(\lambda,\phi,t)} \tag{5}$$

where $\theta'_p=\pi/2-\lambda_p$ for $\lambda_p \geq 0$ and $\theta'_p=\pi/2+\lambda_p$ for $\lambda_p < 0$. This is equivalent to a VGP colatitude calculated with respect to either North Pole or the South Pole, respectively. The standard deviation over time $(\sigma_{P_i}(\lambda,\phi))$ shows the temporal variability of the PSV index which we call the PSV activity. Codes for estimation of the PSV index are available in supporting information.

The use of the absolute value of λ_p allows us to effectively use the L1 norm as a measure of angular deviation from the relevant pole. Combined with M/M_0 it provides an empirical statistic for evaluating both directional and intensity departures of the field from an axial dipole state with strength comparable to the

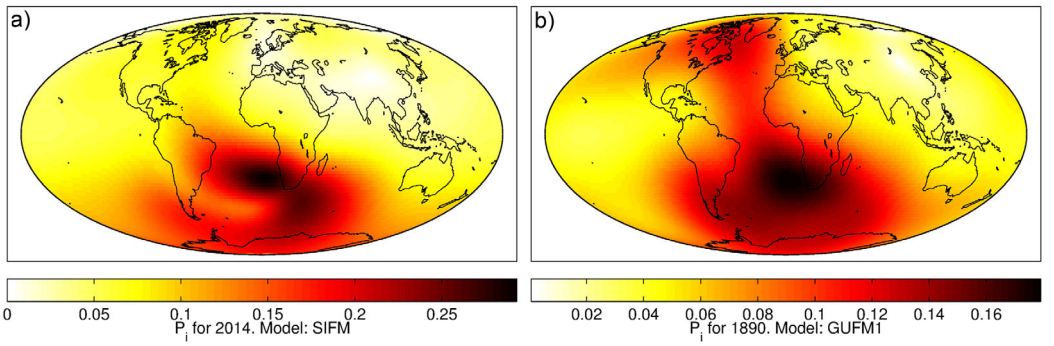

Figure 3. Global PSV index for different models and epochs: (a) SIFM [*Olsen et al.*, 2015] estimated for 2014 and (b) a snapshot of *gufm1* [*Jackson et al.*, 2000] for 1890 AD. Note that the color scales are different, and resolution of the models on different time scales is variable. The maximum PSV indices for these particular models are: 0.3 for SIFM and 0.18 for *gufm1*.

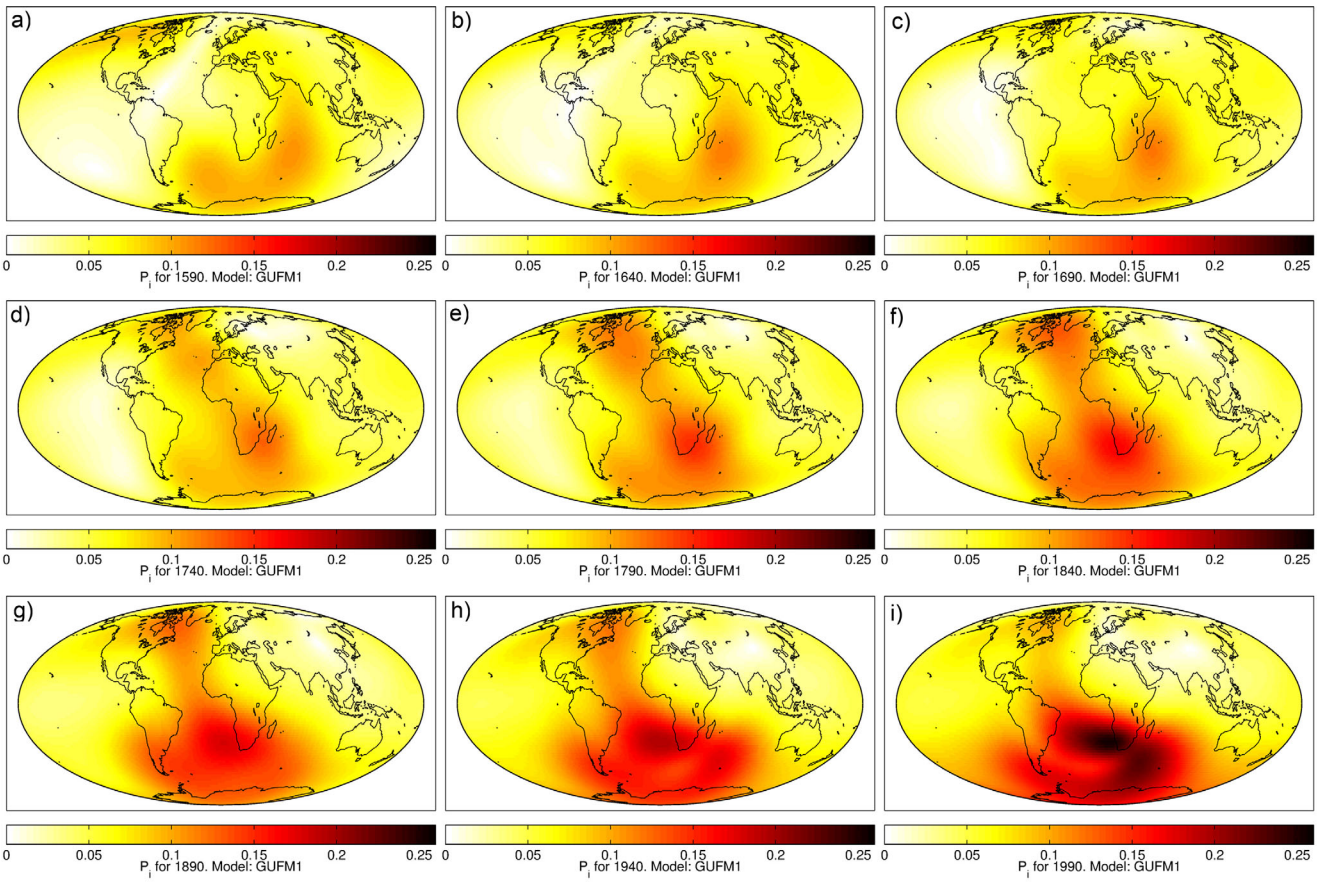

Figure 4. Maps of the PSV index for *gufm1* model from (a) 1590 to (i) 1990, every 50 years. Same color scale applied.

modern field. We envisage using P_i in a variety of ways: (i) geographic variations in P_i identify any unusual spatial structure in the field, e.g., Figure 3; (ii) global time variations, e.g., Figure 4; (iii) analysis of time varying global output from dynamo simulations or paleofield models, Figures 6 and 7; (iv) time variations at a fixed locality, e.g., Figure 8—monitoring the evolution of an excursion or reversal; (v) quantifying the variability in temporal or spatial structure over some time interval through evaluation of σ_{P_i}. Examples are discussed in the next section.

If $\theta'_p = 0$ then $P_i = 0$, if $\theta'_p = 11^\circ$ (the tilt of the geomagnetic dipole today) and the VDM is equal to the present day value then $P_i = 0.06$. When the geomagnetic field exhibits stable secular variation, VGP colatitudes typically lie within 30° of the geographic pole and P_i remains rather small. The PSV index regime diagram is presented in Figure 1 for the full range of expected values of the VGP latitude (−90° to 90°) and VDM ($0.05M_0$ to $3.0M_0$). An excursional geomagnetic field with $\theta'_p = 45^\circ$ and dipole moment of $M = 0.5M_0$ gives P_i of 0.5 (at the intersection of the white lines in Figure 1). PSV index is symmetric about the equator with high values for low VDMs and VGPs in the equatorial range (red area in the regime diagram). High field strengths will produce low values of P_i unless they are also associated with anomalously low VGP latitudes. For example, with the Levantine geomagnetic spike observed around 1000 BC we combined VADM and directional data from *Shaar et al.* [2016] yielding an approximate instantaneous estimate at Megiddo of less than 0.1.

3. Application

3.1. P_i for Modern Field Models

To set a baseline for the PSV index, we analyzed predictions from existing geomagnetic field models on modern and historical time scales, when no excursions and reversals occur. The two components of the PSV

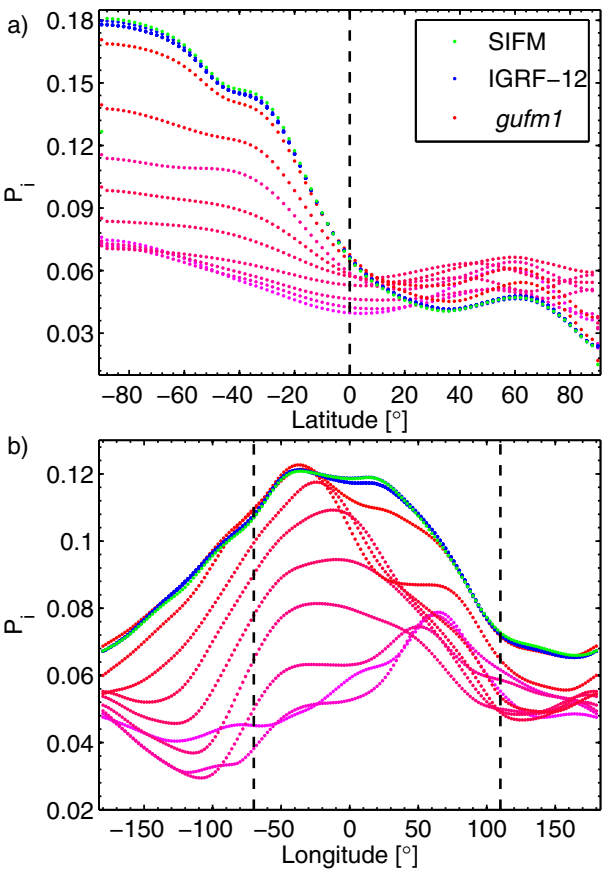

Figure 5. PSV index for three representative models: SIFM (2014), IGRF-12 (2010–2014, 1 year step), and *gufm1* (1590–1990, 50 year steps). PSV indices are averaged every 2 degrees by (a) latitude and (b) longitude. Transitions from red to pink color for the *gufm1* model show the time steps at which model predictions are calculated, from 1990 (red) to 1590 (pink). Dashed lines mark the boundaries between the Northern/Southern hemisphere and Atlantic/Pacific hemisphere. The latter boundary is approximated with 70°W and 110°E.

index, corresponding to the VGP direction (θ'_p/π) and VDM component (M_0/M) in equation (5) are presented separately for the SIFM model [*Olsen et al.*, 2015] in Figure 2. They are combined to provide geographic variations in $P_i(\lambda, \phi)$ for the SIFM model in Figure 3. The epoch 1890 AD for *gufm1* [*Jackson et al.*, 2000] is also presented in Figure 3. As illustrated by these and the next examples, PSV indices for different models show similar geographical variation. The indices have higher values in the Southern than Northern hemisphere and in the Atlantic compared to Pacific Hemisphere. Temporal variation of the index is shown for *gufm1* model at 50 year intervals from 1590 to 1990 (Figure 4). The PSV index is observed to increase over the span of *gufm1* producing a more active Southern hemisphere in recent epochs, but there is probably also an effect from improved model resolution for the more recent times.

The picture becomes clearer when we plot the PSV index distribution as a function of latitude and longitude for selected models (Figure 5). The global maximum of $P_i(\lambda, \phi)$ across the entire time spans of all these models never exceeds the value of 0.3 (0.3 is the maximum for SIFM and IGRF-12 [*Thébault et al.*, 2015] and 0.25 for *gufm1* model). Figure 5 also shows the time variations of the PSV index for *gufm1*. The average index by longitude, for example, decreases in peak value going back in time (in 50 year steps), with the highest values observed for 1990 epoch. Moreover, the peak activity is moving westward from the western Indian Ocean into the South Atlantic, during the period 1590–1990, an observation characteristic of the South Atlantic Anomaly.

3.2. P_i for Dynamo Simulations and a Paleofield Reversal Model

On longer time scales numerical dynamo simulations can be used to generate a complete global representation for P_i, useful for comparing with paleomagnetic observations to assess whether the numerical simulations have Earth-like properties. We used the Glatzmaier-Roberts geodynamo models [*Glatzmaier et al.*, 1999] to present results of excursional and reversal behavior in geodynamo simulations, in particular their model "h" that has an imposed pattern of the radial CMB heat flux based on seismic tomography of the lowermost mantle (Figure 6). This model was chosen as one with some aspects of realistic Earth-like behavior that exhibits geomagnetic excursions in addition to reversals. We analyzed one snapshot from the range of stable secular variation (Model A in Figure 6), two during the transition period of a reversal (Model B and Model C) and one at the peak of a geomagnetic excursion (Model D). The PSV index of Model A reflects a stable field with a mean index of 0.3. During the reversal, the PSV index reaches a maximum of 5 (with a mean value of 1), while for the excursion (Model D) goes up to 82 with a mean of 6. In this particular simulation, the dipole moment during the excursion is about 20 times lower than for the reversal times B and C (Figure 6), which results in a larger index for the excursion. Overall the global mean values of the index during geomagnetic excursions and reversals are greater than 0.5, the proposed limit for characterization of

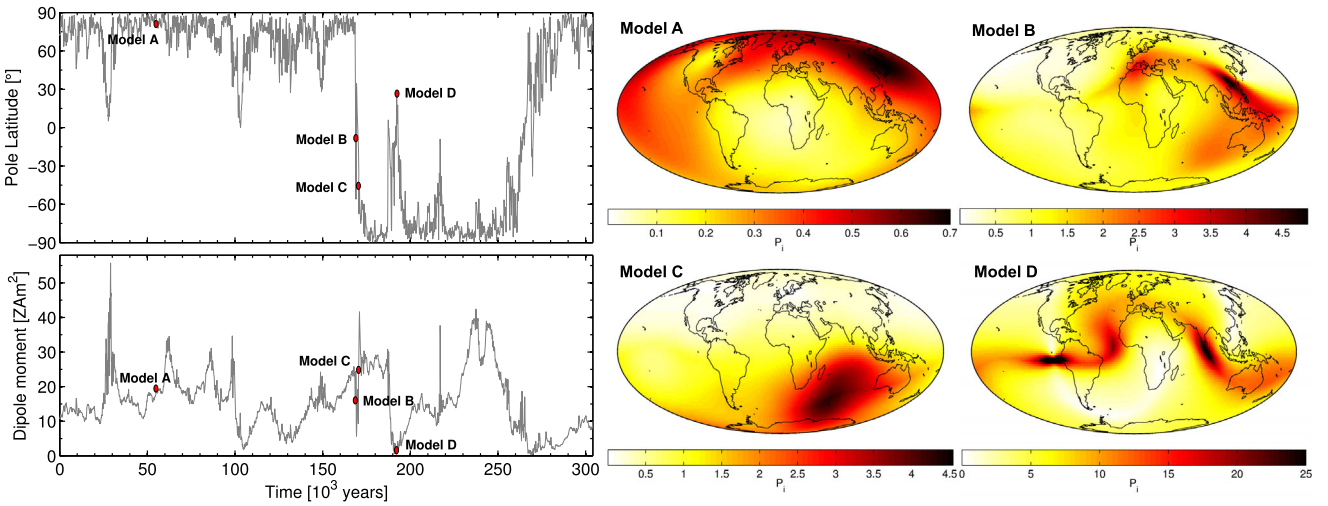

Figure 6. Snapshots of global PSV index for dynamo simulations using Glatzmaier-Roberts geodynamo model "h" in *Glatzmaier et al.* [1999]. This model has an imposed pattern of the radial CMB heat flux based on seismic tomography of the lowermost mantle. Model A: stable geomagnetic field; Models B and C: during a reversal; and Model D: peak of geomagnetic excursion. The time interval between the Models B and C is about 2 kyr. For clarity and better visibility, the color scale for Model D is limited to 25, maximum value is 82.

transitional events. Models B and D show concentrations of activity at lower latitudes, while C appears to be in a somewhat intermediate state, perhaps reflecting the impending recovery of more stable reversed polarity field.

A comparison can be made with a geomagnetic field model during the Matuyama-Brunhes polarity reversal that is based on paleomagnetic data, one loess and 10 deep sea paleomagnetic records [*Ingham and Turner*, 2008] for which P_i also exhibits high values during the reversal period (Figure 7). For instance, in the 34 kyr interval around the time of reversal in the axial dipole coefficient, the PSV index has a mean of 1.2 and reaches a global maximum of 20. Both, the geodynamo simulations and paleomagnetic models, show that intense and active patches of P_i occur during transitional events and they can be distributed across several different and rapidly evolving regions. As in the numerical simulations, peak values tend to be more concentrated at low to midlatitude locations.

3.3. P_i for Sediment Records

We turn now to time series of individual sedimentary paleomagnetic records with stronger PSV signals from the Laschamp excursion and the most recent reversal. A difficulty with sediment magnetic records for calculation of the PSV index is the fact that intensity and declination records are usually in relative, rather than in absolute form. Conversions to VGP latitude (equation (2)) and dipole moment (equation (3)) require absolute declination and relative paleointensity (RPI) calibration, respectively. Robust estimates of the dipole moment and accurate absolute orientation for declination are a major challenge when using sediment paleomagnetic records for paleomagnetic field models [*Panovska et al.*, 2015].

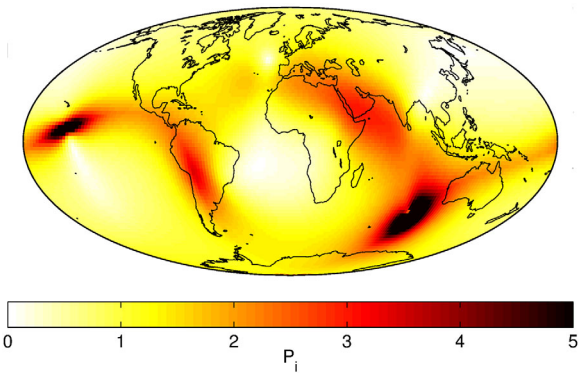

Figure 7. Global PSV index for a geomagnetic model during the Matuyama-Brunhes polarity reversal based on paleomagnetic data [*Ingham and Turner*, 2008]. The snapshot corresponds to the midpoint of the 34 kyr interval spanned by the model, the time when the actual reversal is observed. For better visibility, the color scale is limited to 5. The peak index is 20.

Two examples of the PSV index for sediment data are given in Figure 8, the first (PS2644-5) [*Kissel et al.*, 1999; *Laj et al.*, 2000] spanning the Mono and Laschamp excursions, and the second (ODP 983) [*Channell*, 1999] covers an interval of 250 kyr including the Matuyama

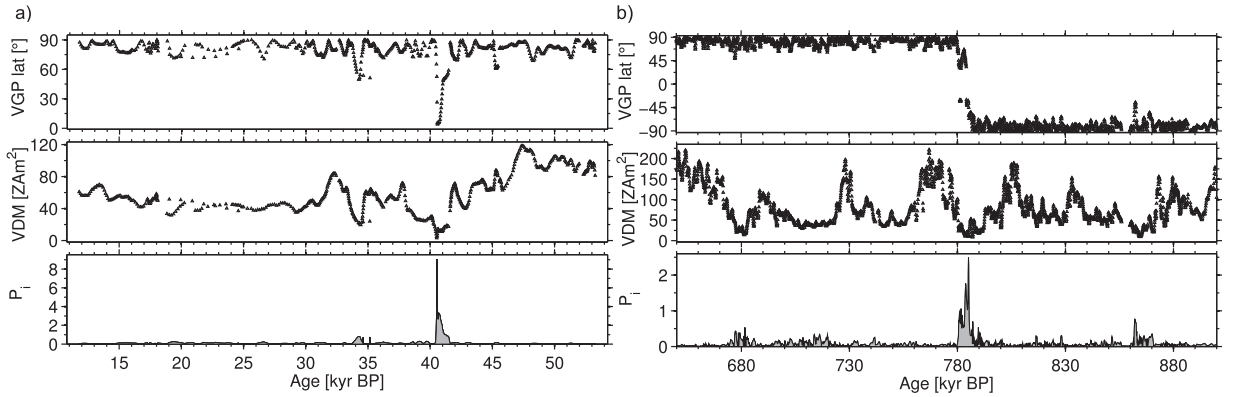

Figure 8. PSV index for two sediment records: (a) PS2644-5, Western Iceland Basin [*Kissel et al.*, 1999; *Laj et al.*, 2000], where peaks in the PSV index are observed at ~41 kyr BP for the Laschamp excursion, and a smaller peak at 34 kyr BP for the Mono Lake excursion; (b) ODP 983, Gardar Drift, Atlantic Ocean [*Channell*, 1999] limited to 650–900 kyr to show only the Matuyama-Brunhes reversal. The maximum value of P_i in this timespan coincides with the reversal at 785 kyr BP.

Brunhes reversal. We calibrated RPI records using the penalized least squares spline fit to a global compilation of VDMs from archeomagnetic and lava flows data covering the past 100 kyr. These data are compiled in the GEOMAGIA.v3, archeological and volcanic database [*Brown et al.*, 2015] and PSV10 database [*Cromwell et al.*, 2012]. We tested the impact of using different overlapping intervals with the absolute dipole moment spline fit for calibration of PS2644-5 record (Figure 8), and estimated a range for the PSV index varying from 6.8 to 9.0 for the Laschamp excursion. The average PSV index changes only slightly, from 0.15 to 0.2.

Because absolute declination is rarely available for sediments, we assume declination equals zero throughout the whole sediment record (equation (2)). This introduces an error in the PSV index that depends on the estimated VGP. This difference is insignificant during stable secular variation, when declination is small, and increases when the field starts to change polarity. For instance, P_i of the Mono Lake excursion recorded in the paleomagnetic record PS2644-5 at 34.3 kyr BP varies from 0.8 (D=0°) to 1.7 (D=180°). The Laschamp excursion has a peak P_i of 9 at 40.54 kyr BP, under the assumption of $D = 0$. The index increases to 12.2 if declination is set to 90° and 10.3 for declination of 180°. This compromise allows more records to be included in the analysis, and is particularly useful for global studies of the new compilation of 100 kyr paleomagnetic sediment records [*Panovska and Constable*, 2015] which contains more intensity and inclination compared to declination data. It is also worth noting that declination paleomagnetic records in the 100 kyr data compilation as well as in the Holocene appeared to be the least reliable component based on uncertainty analyses [*Panovska et al.*, 2012]. However, when full vector absolute paleomagnetic and archeomagnetic data are available, these are of course preferable for the P_i analysis. A strategy that might have value under some circumstances would be setting the average declination to zero, as is often done in invoking the geocentric axial dipole hypothesis for the average field.

As in the numerical simulations, we find that P_i peaks more strongly during the Laschamp excursion than during the Matuyama-Brunhes reversal. The signature of the Mono Lake excursion is much weaker (maximum value of 0.8 at 34.3 kyr), but still reaches past the threshold value of 0.5. During excursions, the peak in the PSV index is observed when a sharp directional change occurs (Figure 8) since the intensity decreases more gradually over a longer period than the rapid directional change. Duration of the Laschamp excursion defined by P_i values above 0.5 (Figure 8a) is 1 kyr, while the time periods confined by the conventional limits $M/M_0 < 0.5$ and $\theta'_p < 45°$ are 3.5 and 0.5 kyr, respectively. The length of the Matuyama-Brunhes transition recorded in ODP 983 is about 5 kyr estimated by $P_i > 0.5$ (Figure 8b) whereas $M/M_0 < 0.5$ and $-45° < \theta'_p < 45°$ criteria give different durations of 12 and 4.7 kyr, respectively.

Factors that influence the recording fidelity of sediments, such as sedimentation rate and postdepositional processes, also affect the PSV index estimation. The absence of specific sharp geomagnetic field changes in some sediment records can be attributed to smoothing by the sedimentary remanence acquisition process and low sedimentation rates. Depending on the degree of smoothing, the transitional VGP positions

represent time-integrated records of the excursions. This does complicate the identification and discrimination of excursional events and the PSV index values of geomagnetic excursions will inevitably be attenuated in some sediment records.

4. Conclusions

Variability in intensity and relative dispersion of directions or pole positions have previously been used to quantify PSV. By combining the two, we provide an index for PSV evaluation that is flexible enough to be used on individual time series at local, regional and global scales, time-varying geomagnetic fields and snapshots, and is even suitable for statistical analyses based on lava flow directional and paleointensity data. In previous analyses, the separation of stable PSV from an intermediate/transitional geomagnetic regime depended on the selected cut-off VGP latitude or threshold for intensity/dipole moment variations. The new PSV index represents a broad continuum of field behavior including excursions and reversals. By analyzing modern and historical geomagnetic field models, and longer time-scale paleomagnetic sediment records, we were able to distinguish between stable and transitional field behavior. The new P_i index also provides a unified approach to determining how long the excursion/reversal transition lasts.

Based on the SIFM model, the current maximum PSV index is observed in the South Atlantic ($P_i = 0.3$) with a minimum regional dipole moment of half the present-day value M_0. Separating the strength (M_0/M) and directional contributions (θ'_p/π) to the PSV index (Figure 2) we can find that they occur at different locations, with the latter appearing in the high southern latitudes. The maximum index of 0.3 for the SIFM model corresponding to the SAA is significantly smaller than that estimated for the most recent excursions, and more than an order of magnitude lower than that obtained for the PS2644-5 sediment record of the Laschamp, the best recorded excursion over the past 100 kyr. Both simulated and paleomagnetic records exhibit localized values of P_i that can be higher for excursions than reversals in our analyses. Although the present-day modern data have higher resolution than paleomagnetic sediment data, the observed difference in the PSV index is significant, and the SAA value lies well within the stable SV range, far from the excursions and reversal area in the regime diagram (Figure 1). Finally, we note that in the context of changes in reversal rate, especially for higher than normal rates we expect that the accompanying dips in intensity and large directional variations will produce higher overall values for P_i and its variability.

Acknowledgments

This work has been supported under NSF grant EAR 1246826. We thank Monika Korte for useful suggestions and the Helmholtz Zentrum Potsdam—Deutsches GFZ for their hospitality during our collaboration on this work. We are grateful to three anonymous reviewers who provided suggestions for improving structure and clarity of the manuscript. Sediment magnetic records are available online via MagIC (http://earthref.org/MAGIC/) and Pangea (http://www.pangaea.de/) databases. Models available upon request to panovska@gfz-potsdam.de.

References

Brown, M. C., F. Donadini, M. Korte, A. Nilsson, K. Korhonen, A. Lodge, S. N. Lengyel, and C. G. Constable (2015), GEOMAGIA50.v3: 1. General structure and modifications to the archeological and volcanic database, *Earth Planets Space*, *67*, 83, doi:10.1186/s40623-015-0232-0.

Butler, R. F. (1992), *Paleomagnetism: Magnetic Domains to Geologic Terranes*, Blackwell Sci., Boston.

Channell, J. E. T. (1999), Geomagnetic paleointensity and directional secular variation at Ocean Drilling Program (ODP) Site 984 (Bjorn Drift) since 500 ka: Comparisons with ODP Site 983 (Gardar Drift), *J. Geophys. Res.*, *104*(B10), 22,937–22,951.

Coe, R. S., and G. A. Glatzmaier (2006), Symmetry and stability of the geomagnetic field, *Geophys. Res. Lett.*, *33*, L21311, doi:10.1029/2006GL027903.

Constable, C. G. (2003), Geomagnetic reversals: Rates, timescales, preferred paths, statistical models and simulations, in *Earth's Core and Lower Mantle*, edited by C. A. Jones, A. M. Soward, and K. Zhang, pp. 77–99, Taylor and Francis, London, U. K.

Constable, C. G. (2007), Dipole moment variation, in *Encyclopedia of Geomagnetism and Paleomagnetism*, edited by D. G. Gubbins and E. Herrero-Bervera, pp. 159–161, Springer, Dordrecht, Netherlands.

Constable, C. G., M. Korte, and S. Panovska (2016), Persistent high paleosecular variation activity in southern hemisphere for at least 10000 years, *Earth Planet. Sci. Lett.*, *453*, 78–86.

Cromwell, G., L. Tauxe, N. A. Jarboe, C. L. Johnson, and C. G. Constable (2012), Paleosecular variation over the last 10 Ma from a new global dataset (PSV10): Evidence for long-term hemispheric asymmetry, Abstract GP11A-07 presented at 2012 Fall Meeting, AGU, San Francisco, Calif.

Cromwell, G., L. Tauxe, H. Staudigel, C. G. Constable, A. A. P. Koppers, and R. Pedersen (2013), In search of long-term hemispheric asymmetry in the geomagnetic field: Results from high northern latitudes, *Geochem. Geophys. Geosyst.*, *14*, 3234–3249, doi:10.1002/ggge.20174.

Cromwell, G., L. Tauxe, and S. A. Halldórsson (2015), New paleointensity results from rapidly cooled Icelandic lavas: Implications for Arctic geomagnetic field strength, *J. Geophys. Res. Solid Earth*, *120*, 2913–2934, doi:10.1002/2014JB011828.

Davis, T. N., and M. Sugiura (1966), Auroral electrojet activity index *AE* and its universal time variations, *J. Geophys. Res.*, *71*(3), 785–801.

De Santis, A., and E. Qamili (2015), Geosystemics: A systemic view of the Earth's magnetic field and the possibilities for an imminent geomagnetic transition, *Pure Appl. Geophys.*, *172*, 75–89.

Glatzmaier, G. A., R. S. Coe, L. Hongre, and P. H. Roberts (1999), The role of the earth's mantle in controlling the frequency of geomagnetic reversals, *Nature*, *401*, 885–890.

Hulot, G., C. Eymin, B. Langlais, M. Mandea, and N. Olsen (2002), Small-scale structure of the geodynamo inferred from Oersted and Magsat satellite data, *Nature*, *416*, 620–623.

Ingham, M., and G. Turner (2008), Behaviour of the geomagnetic field during the Matuyama-Brunhes polarity transition, *Phys. Earth Planet. Inter.*, *168*, 163–178, doi:10.1016/j.pepi.2008.06.008.

Jackson, A., A. R. T. Jonkers, and M. R. Walker (2000), Four centuries of geomagnetic secular variation from historical records, *Philos. Trans. R. Soc. London A*, *358*, 957–990.

Kissel, C., C. Laj, L. Labeyrie, T. Dokken, A. Voelker, and D. Blamart (1999), Rapid climatic variations during marine isotopic stage 3: Magnetic analysis of sediments from Nordic Seas and North Atlantic, *Earth Planet. Sci. Lett.*, *171*, 489–502.

Laj, C., C. Kissel, A. Mazaud, J. E. T. Channell, and J. Beer (2000), North Atlantic paleointensity stack since 75 ka (NAPIS-75) and the duration of the Laschamp event, *Philos. Trans. R. Soc. London A*, *358*, 1009–1025.

Love, J. J., and K. J. Remick (2007), Magnetic indices, in *Encyclopedia of Geomagnetism and Paleomagnetism*, edited by D. G. Gubbins and E. Herrero-Bervera, pp. 509–512, Springer, Dordrecht, Netherlands.

Lu Lin, J., K. L. Verosub, and A. P. Roberts (1994), Decay of the virtual dipole moment during polarity transitions and geomagnetic excursions, *Geophys. Res. Lett.*, *21(7)*, 525–528.

Mayaud, P. N. (1980), *Derivation, Meaning, and Use of Geomagnetic Indices, Geophys. Monogr. Ser.*, vol. 22, AGU, Washington, D. C.

McFadden, P. L., R. T. Merrill, and M. W. McElhinny (1988), Dipole/quadrupole family modeling of paleosecular variation, *J. Geophys. Res.*, *93*(B10), 11,583–11,588.

McFadden, P. L., R. T. Merrill, M. W. McElhinny, and S. Lee (1991), Reversals of the Earth's magnetic field and temporal variations of the dynamo families, *J. Geophys. Res.*, *96*(B3), 3923–3933.

Menvielle, M., and A. Berthelier (1991), The K-derived planetary indices: Description and availability, *Rev. Geophys.*, *29*(3), 415–432.

Merrill, R. T., M. W. McElhinny, and P. L. McFadden (1996), *The Magnetic Field of the Earth: Paleomagnetism, the Core, and the Deep Mantle*, Academic, San Diego, Calif.

Olsen, N., H. Lühr, T. J. Sabaka, M. Mioara, M. Rother, L. Tøffner-Clausen, and S. Choi (2006), CHAOS—A model of the Earth's magnetic field derived from CHAMP, Ørsted, and SAC-C magnetic satellite data, *Geophys. J. Int.*, *166*, 67–75.

Olsen, N., et al. (2015), The Swarm Initial Field Model for the 2014 geomagnetic field, *Geophys. Res. Lett.*, *42*, 1092–1098, doi:10.1002/2014GL062659.

Olson, P., P. Driscoll, and H. Amit (2009), Dipole collapse and reversal precursors in a numerical dynamo, *Phys. Earth Planet. Inter.*, *173*, 121–140.

Olson, P. L., and U. R. Christensen (2006), Dipole moment scaling for convection-driven planetary dynamos, *Earth Planet. Sci. Lett.*, *250*, 561–571.

Panovska, S., and C. G. Constable (2015), Global geomagnetic field mapping—From secular variation to geomagnetic excursions, *EGU*, *17*, Abstract EGU2015-8159-1.

Panovska, S., C. C. Finlay, F. Donadini, and A. M. Hirt (2012), Spline analysis of Holocene sediment magnetic records: Uncertainty estimates for field modelling, *J. Geophys. Res.*, *117*, B02101, doi:10.1029/2011JB008813.

Panovska, S., M. Korte, C. C. Finlay, and C. G. Constable (2015), Limitations in paleomagnetic data and modelling techniques and their impact on Holocene geomagnetic field models, *Geophys. J. Int.*, *202*, 402–418, doi:10.1093/gji/ggv137.

Shaar, R., L. Tauxe, H. Ron, Y. Ebert, S. Zuckerman, I. Finkelstein, and A. Agnon (2016), Large geomagnetic field anomalies revealed in Bronze to Iron Age archeomagnetic data from Tel Megiddo and Tel Hazor, Israel, *Earth Planet. Sci. Lett.*, *442*, 173–185.

Singer, B. S. (2014), A Quaternary geomagnetic instability time scale, *Quat. Geochronol.*, *21*, 29–52.

Sugiura, M. (1964), Hourly values of equatorial *Dst* for the IGY, *Ann. Int. Geophys. Year*, *35*, 9–45.

Thébault, E., et al. (2015), International Geomagnetic Reference Field: The 12th generation, *Earth Planets Space*, *67*, 79, doi:10.1186/s40623-015-0228-9.

Wicht, J., S. Stellmach, and H. Harder (2009), Numerical models of the geodynamo: From fundamental Cartesian models to 3D simulations of field reversals, in *Geomagnetic Field Variations*, edited by K. H. Glassmeier, H. Soffel, and J. F. W. Negendank, pp. 107–158, Springer, Berlin, doi:10.1007/978-3-540-76939-2_4.

Ziegler, L. B., and C. G. Constable (2015), Testing the geocentric axial dipole hypothesis using regional paleomagnetic intensity records from 0–300 ka, *Earth Planet. Sci. Lett.*, *423*, 48–56, doi:10.1016/j.epsl.2015.04.022.